

# Journal of Visualized Experiments

## Atom Probe Tomography (APT) Analysis of Exsolved Mineral Phases

--Manuscript Draft--

<b>Article Type:</b>	Invited Methods Article - JoVE Produced Video
<b>Manuscript Number:</b>	JoVE59863R3
<b>Full Title:</b>	Atom Probe Tomography (APT) Analysis of Exsolved Mineral Phases
<b>Keywords:</b>	Atom probe tomography (APT); geochemistry; mineralogy; volcanology; Microscopy; Earth Sciences
<b>Corresponding Author:</b>	Alberto Perez-Huerta, Ph.D. University of Alabama Tuscaloosa, Alabama UNITED STATES
<b>Corresponding Author's Institution:</b>	University of Alabama
<b>Corresponding Author E-Mail:</b>	aphuerta@ua.edu
<b>Order of Authors:</b>	Kimberly Genareau Alberto Perez-Huerta, Ph.D. Fernando Laiginhas
<b>Additional Information:</b>	
<b>Question</b>	<b>Response</b>
Please indicate whether this article will be Standard Access or Open Access.	Standard Access (US\$2,400)
Please indicate the <b>city, state/province, and country</b> where this article will be <b>filmed</b> . Please do not use abbreviations.	Tuscaloosa, Alabama, USA



April 18, 2019

Dear Dr. DSouza [Editor JoVE],

Thank you for your additional editorial comments. Please find enclosed with this letter the revised version of the second revision "R2" of the article entitled "Atom Probe Tomography (APT) Analysis of Exsolved Mineral Phases" towards publication in *JoVE*.

We have considered carefully your comments, and we have determined that, for "APT Data Processing", software steps are difficult to be better explained with more words in order to be adequate for scripting and filming. Thus, we followed your recommendation after the first revision of the manuscript and remove the highlighting in this section; if, during filming, it is considered showing this aspect of the protocol, we will be glad to collaborate towards this goal.

Thank you very much for your time and consideration. We hope that changes are already adequate for acceptance of the manuscript.

Sincerely yours,

Alberto Perez-Huerta (On behalf of the authors)

Associate Professor  
Dept. of Geological Sciences  
The University of Alabama

**TITLE:**

Atom Probe Tomography Analysis of Exsolved Mineral Phases

**AUTHORS AND AFFILIATIONS:**

Kimberly Genareau<sup>1</sup>, Alberto Perez-Huerta<sup>1</sup>, Fernando Laiginhas<sup>1</sup>

<sup>1</sup>Department of Geological Sciences, University of Alabama, Tuscaloosa, Alabama, USA

**Corresponding Authors:**

Kimberly Genareau (kdg@ua.edu)

Alberto Perez-Huerta (aphuerta@ua.edu)

**Email Addresses of Co-Authors:**

Fernando Laiginhas (ftlaiginhas@ua.edu)

**KEYWORDS:**

Atom probe tomography, APT, volcanic ash, titanomagnetite, ilmenite, exsolution lamellae, FIB-SEM lift-out, LEAP

**SHORT ABSTRACT:**

Analysis of the morphology, composition, and spacing of exsolution lamellae can provide essential information to understand geological processes related to volcanism and metamorphism. We present a novel application of APT for the characterization of such lamellae and compare this approach to the conventional use of electron microscopy and FIB-based nanotomography.

**LONG ABSTRACT:**

Element diffusion rates and temperature/pressure control a range of fundamental volcanic and metamorphic processes. Such processes are often recorded in lamellae exsolved from host mineral phases. Thus, the analysis of the orientation, size, morphology, composition and spacing of exsolution lamellae is an area of active research in the geosciences. The conventional study of these lamellae has been conducted by scanning electron microscopy (SEM) and transmission electron microscopy (TEM), and more recently with focused ion beam (FIB)-based nanotomography, yet with limited chemical information. Here, we explore the use of atom probe tomography (APT) for the nanoscale analysis of ilmenite exsolution lamellae in igneous titanomagnetite from ash deposits erupted from the active Soufrière Hills Volcano (Montserrat, British West Indies). APT allows the precise calculation of interlamellar spacings ( $14\text{--}29 \pm 2$  nm) and reveals smooth diffusion profiles with no sharp phase boundaries during the exchange of Fe and Ti/O between the exsolved lamellae and the host crystal. Our results suggest that this novel approach permits nanoscale measurements of lamellae composition and interlamellar spacing that may provide a means to estimate the lava dome temperatures necessary to model extrusion rates and lava dome failure, both of which play a key role in volcanic hazard mitigation efforts.

**INTRODUCTION:**

The study of chemical mineralogy has been a major source of information within the field of Earth Sciences for more than a century, as minerals actively record geological processes during and after their crystallization. Physio-chemical conditions of these processes, such as temperature changes during volcanism and metamorphism, are recorded during mineral nucleation and growth in the form of chemical zonation, striations, and lamellae, among others. Exsolution lamellae form when a phase unmixes into two separate phases in the solid state. The analysis of the orientation, size, morphology, and spacing of such exsolution lamellae can provide essential information to understand temperature and pressure changes during volcanism and metamorphism<sup>1-3</sup> and the formation of ore mineral deposits<sup>4</sup>.

Traditionally, the study of exsolution lamellae was conducted with the observation of micrographs by simple scanning electron imaging<sup>5</sup>. More recently, this has been substituted by the use of energy-filtered transmission electron microscopy (TEM) providing detailed observations at the nanoscale level<sup>1-3</sup>. Nevertheless, in both cases, the observations are made in two dimensions (2D), which is not fully adequate for three dimensional (3D) structures represented by these exsolution lamellae. Nanotomography<sup>6</sup> is emerging as a new technique for the 3D observation of nanoscale features inside minerals grains, yet there is insufficient information about the composition of these features. An alternative to these approaches is the use of atom probe tomography (APT), representing the highest spatial resolution analytical technique in existence for the characterization of materials<sup>7</sup>. The strength of the technique lies in the possibility of combining a 3D reconstruction of nanoscale features with their chemical composition at the atomic scale with a near part-per-million analytical sensitivity<sup>7</sup>. Previous applications of APT to the analysis of geological samples have provided excellent results<sup>8-11</sup>, particularly in the chemical characterization of element diffusion and concentrations<sup>9, 12-13</sup>. Yet, this application has not been used for the study of exsolution lamellae, abundant in some minerals hosted in metamorphic and igneous rocks. Here, we explore the use of APT, and its limitations, for the analysis of the size and composition of exsolution lamellae, and interlamellar spacing in volcanic titanomagnetite crystals.

## **PROTOCOL:**

### **1. Sourcing, selection, and preparation of mineral grains**

NOTE: Samples were obtained from the catalogued collection at the Montserrat Volcano Observatory (MVO) and derived from falling deposits originating from a vigorous ash venting episode at Soufrière Hills Volcano that occurred on 5 October, 2009; this was one of 13 similar events over a course of three days<sup>14</sup>. This ash venting preceded a new phase of lava dome growth (phase 5) that commenced on 9 October. Previous analysis of this sample showed it to be a combination of dense dome rock fragments, glassy particles, and accidental lithics<sup>14</sup>.

**1.1) Pour 1 g of volcanic ash sample into a 10 cm diameter glass Petri dish.**

**1.2) Wrap a small (3 cm x 3 cm) sheet of weighing paper around a 10 G magnet.**



1.4) Use a paper-wrapped magnet to pull magnetite-rich grains between 100  $\mu\text{m}$  and 500  $\mu\text{m}$  in diameter from the ash sample and place in a 32  $\mu\text{m}$  (5  $\phi$ ), 8 cm diameter stainless-steel sieve.

1.5) Rinse in deionized water for 20–30 s using a squeeze bottle to remove smaller, adhering ash particles (which will pass through the sieve), and air-dry for 24 h.

1.6) Affix clean and dry ash particles to sample mounts suitable for the secondary electron microscope (SEM). Image in secondary electron mode at a 15–20 kV accelerating voltage and at a working distance of 10 mm to select the 5–10 best candidates for further analysis. Selected grains should be predominantly (>50%) magnetite (**Figure 1a,b**).

1.7) Affix selected ash grains to clear tape, surround with one-inch diameter hollow mold (metal, plastic, or rubber) that has been internally coated with vacuum grease, and pour in epoxy resin to fill the mold (2  $\text{cm}^3$ ). Allow epoxy to cure according to the specific epoxy instructions.

1.8) Once epoxy has cured, remove from mold and peel tape from the bottom. Ash grains should be partially exposed.

1.9) Polish the epoxy-cast ash grains using SiC grinding paper of five different grit sizes (400, 800, 1200, 1500 and 2000 grit).

1.9.1) Polish the sample with each grit size, from highest (400) to lowest (2000) in a figure eight motion for at least 10 min. In between grit sizes, sonicate the sample in a bath of deionized water for 10 min.

1.9.2) Check the sample under a microscope to ensure that the polishing grit is not present, and the sample surface is free from scratches. If scratches are present, repeat the polishing procedure with the previous grit size before sonicating and moving to the next grit size.

1.10) Polish the epoxy-cast ash grains with alumina polishing suspensions of 1.0  $\mu\text{m}$  and then 0.3  $\mu\text{m}$  on polishing cloths.

1.10.1) Polish the sample with each suspension in a figure eight motion for at least 10 min. In between suspension sizes, sonicate the sample in a bath of deionized water for 10 min.

1.10.2) Check the sample under a microscope to ensure that the suspension is not present and the sample surface is free of scratches. If scratches are present, repeat the polishing procedure with the previous suspension before sonicating and moving to the next suspension size. At the end of the polishing procedure, the epoxy surface should be smooth and the ash grains should be flat and well-exposed.

1.11) Coat the sample surface with a conducting coat of ~10 nm thick carbon using an available sputter coating device.

1.12) Obtain backscattered electron images of the ash grains with the electron microscope at a 15–20 kV accelerating voltage and a working distance of 10 mm to determine the location of exsolution lamellae in the magnetite (**Figure 1c**), as conducted in previous studies<sup>5</sup>.

[Place Figure 1 here]

## 2. Atom probe tomography (APT) sample preparation

2.1) APT samples will be prepared from a wedge of material that reveals the presence of exsolution lamellae (**Figure 1d**) employing a FIB-based lift-out protocol<sup>16</sup> (**Figure 2**). Prior to FIB work, sputter coat the sample surface with 15 nm layer of Cu to avoid electron charging and sample drifting.

2.2) Using a focused ion beam in a dual beam scanning electron microscope (FIB-SEM), deposit a rectangle of platinum (Pt) (3  $\mu\text{m}$  in thickness) on the polished section of interest containing the lamellae over a 1.5  $\mu\text{m}$  x 20  $\mu\text{m}$  region using a gallium ( $\text{Ga}^+$ ) ion beam at 30 kV and 7 pA.

NOTE: This platinum layer is deposited to protect the region of interest (ROI) from ion beam damage.

2.3) Mill three wedges of material below three sides of the Pt rectangle using the ion beam (30 kV, 1 nA). See **Figure 1d** and **Figure 2**.

2.4) Insert the gas injection system (GIS) and weld the wedge to an in situ nano-manipulator using GIS-deposited Pt before cutting the final edge free (**Figure 2a**).

2.4) Using the  $\text{Ga}^+$  ion beam (5 kV and 240 pA), cut ten 1–2  $\mu\text{m}$  wide segments from the wedge and sequentially affix them with Pt to the tops of Si posts of a microtip array coupon (**Figure 2b–d**).

2.5) Shape and sharpen each specimen tip using annular milling patterns of increasingly smaller inner and outer diameters (**Figure 3**). Initially, perform the milling at 30 kV to produce the specimen geometry necessary for APT (**Figure 3**, left panel).

2.6) Perform the final milling at an accelerating voltage of 5 kV in order to reduce  $\text{Ga}^+$  implantation and obtain a consistent tip-to-tip shape (**Figure 3**, right panel).

2.7) By applying the measuring tools of the SEM to the figure, ensure that the diameter at the top of the tips ranges 50–65 nm, while the shank angle of the tips ranges from 25° to 38°.

NOTE: Further details have been previously published, describing the conventional lift-out protocol<sup>16</sup>.

[Place Figures 2 and 3 here]

### 3. APT data acquisition

3.1) Perform analysis with a local electrode atom probe (LEAP) equipped with a pico-second 355 nm UV laser. See specific LEAP running parameters in **Table 1**.

NOTE: Analyses were performed with a LEAP equipped with a pico-second 355 nm UV laser, housed in the Central Analytical Facility (CAF) at The University of Alabama.

3.2) Mount the micro-coupon with the sharpened tips, welded to the Si posts, in a specimen puck and load into a carousel for placement inside the LEAP.

3.3) Insert the carousel inside the buffer chamber of the LEAP.

3.4) Turn the laser head on and perform a laser calibration.

3.5) After achieving vacuum in the analysis chamber at or below  $6 \times 10^{-11}$  Torr, insert the puck specimen into the main analysis chamber. For this use a transfer rod; this is operated with a series of automatic steps and manual insertion.

3.6) Before analysis, select the tip by moving the specimen puck to align the micro-coupon with the local electrode and update the database to indicate the tip number.

NOTE: Four out of six tips were analyzed successfully (two fractured during analysis) and resulted in a variable amount of acquired data ranging from 26 to 92 million total detected ions, which corresponded to the removal of a 160–280 nm-thick layer of magnetite (see specific LEAP running parameters in **Table 1**).

[Place Table 1 here]

### 4. APT data processing

4.1) Open the dataset in the processing software (see the **Table of Materials**) and perform the following steps for data analysis.

4.1.1. Review the information setup.

4.1.2. Select ion sequence range based on the voltage history plot. Select the detector region of interest (ROI).

4.1.3. Perform time-of-flight (TOF) correction. Use peaks corresponding to oxygen and iron for the TOF correction.

4.1.4. Perform mass calibration with the identification of main peaks.

4.1.5. Perform the ranging of ions for their assignments to specific masses.

4.1.6. Perform the reconstruction of the tip profile.

4.2) Show the data into the two main formats: 1) mass-to-charge state ratio (Da) chemical spectra (**Figure 4**); and 2) 3D reconstructions of tip specimens (**Figure 5**).

4.3) Define peak ranges as the entire visible peak, or adjust manually when large thermal tails are present, for each mass-to-charge state ratio spectrum (**Figure 4**). These peaks represent single elements or molecular species, and the decomposition of peaks provides the overall chemical composition for each tip or feature (i.e., clusters and exsolution lamellae) inside each tip (**Table 2**).

4.4) Perform three-dimensional (3D) tip reconstructions using the “voltage” tip profile method<sup>17</sup> to determine the reconstructed radius as a function of analyzed depth (**Figure 5** and **Movie 1**).

4.5) Reconstruct isosurfaces of exsolution lamellae to conduct interlamellar spacing measurements (**Figure 5**) and establish the host mineral-lamella chemical relationship using proxigrams<sup>17-18</sup> (**Figure 6**).

4.6) Measure interlamellar spacings with image analysis software.

[Place Figure 4 and Table 2 here]

## REPRESENTATIVE RESULTS:

Like many titanomagnetite crystals from various stages of the Soufrière Hills Volcano (SHV) eruption, the crystal analyzed here contains exsolution lamellae <10  $\mu\text{m}$  in thickness, visible in secondary SEM images (**Figure 1d**), which separate zones of Ti-rich magnetite, indicating a C2 stage of oxidation<sup>18</sup>. Based upon the SEM images, spacing between these lamellae ranges from 2 to 6  $\mu\text{m}$  ( $n = 15$ ). Four titanomagnetite specimen tips, referred as 207, 217, 218, and 219, were successfully extracted from this single crystal and analyzed by APT (**Figure 5**). Two of the specimens (207 and 218) showed homogenous concentrations of both Fe and Ti throughout (**Figure 5a**), indicating that lamellae were not intersected. The other two specimens (217 and 219) showed zones with variable concentrations in Fe, O, and Ti (**Figure 5b–e**). These features are parallel to each other and have tapered terminations, indicative of trellis ilmenite<sup>18</sup>. Specimen 219 contains a larger proportion of the intersected lamellae than specimen 217. 3D reconstructions of the APT data (**Figure 5c–e**, **Movie 1**) permit a precise measurement of the interlamellar spacing ( $\lambda$ ) and provide length scales that average 29 nm for specimen 219 ( $n = 30$ ) and 14 nm for specimen 217 ( $n = 15$ ), with a  $1\sigma$  value of 2 nm for both. In addition to these measurements, APT permits extraction of chemical information across these lamellae at high spatial resolution (nanoscale) through the analysis of proxigrams, taking the point 0 as the intersection between the lamella and the host mineral (**Figure 6**). Proxigram diffusion profiles through these zones are smooth. Atomic concentrations of Ti in the crystal, 17% in specimen 217

and 16.5% in specimen 219 (**Figure 6**), confirm that it is a titanomagnetite and are consistent with previous petrologic analyses of SHV eruptive products<sup>18</sup>. These proxigrams also confirm that the composition of lamellae matches that of ilmenite (**Figure 6**).

[Place Figures 5 and 6 here]

## FIGURE AND TABLE LEGENDS:

**Figure 1: Example of magnetite-rich ash grains from venting episodes at the Soufrière Hills volcano.** (a, b): Backscattered electron images (BSE) of both reacted and unreacted textures in magnetite grains. (c) BSE image of a polished magnetite grain showing the presence of exsolution lamellae (light grey laths; red arrows) of potential ilmenite composition. (d) Secondary electron image of a polished magnetite grain prepared for atom probe tomography (APT) analysis, showing the location of some exsolution lamellae (dashed red lines), which are distributed all along the grain surface, and the location of the wedge extraction (blue arrow).

**Figure 2: Example of FIB-SEM sample preparation protocol for APT analysis.** (a) Wedge (W) lift-out extraction with the nanomanipulator (Nm). (b) Lateral view of the micro-coupon array of silicon posts mounted on a copper clip. (c) Top view of the micro-coupon array of silicon posts showing the nanomanipulator for mounting the wedge sections. (d) Wedge fragment (S), showing a portion of the protective platinum cap (Ptc), mounted on a silicon post after welding with platinum (Ptw).

**Figure 3: Example of tips prepared for APT analysis.** (Left) Image of tip after the first stage of sharpening. (Right) Image of the same tip after low kV cleaning, indicating the tip radius (67.17 nm) and the shank angle (26°).

**Figure 4: Example of a representative APT mass-to-charge spectrum.** Spectrum for the analyzed magnetite crystal with individual ranged peaks showing examples of the identification of peaks corresponding to single elements (e.g., oxygen (O) or iron (Fe)) or molecules (e.g., FeO).

**Figure 5: Example of 3D atomic reconstructions of magnetite tips analyzed (z values in nm).** (a) Specimen 218, showing homogenous concentrations of O, Fe, and Ti. (b) Specimen 219, displaying regions depleted in Fe and enriched in O and Ti (lighter areas). (c) Elemental isoconcentration surfaces of specimen 219, showing intralamellar concentrations of Fe < 30.0% in blue, Ti > 25.0% in yellow, and O < 51.5% in purple. (d) View of same area in panel c, but rotated 90° to reveal the measured lamellar spacing ( $\lambda$ ). (e) Specimen 217, showing a relatively smaller portion of exsolution lamellae in the lower left (intralamellar concentrations: Fe < 19.0%, Ti > 33.0%, O < 49.0%).

**Figure 6: Proxigrams of APT data showing atomic concentrations of O, Fe and Ti in specimens 217 and 219, respectively.** A distance of zero on the x-axis (dashed vertical line) represents the boundary between the titanomagnetite on the left and the ilmenite lamellae on the right. Across this boundary, Ti concentrations increase from 17.0% to 44.0% and from 16.5% to 42.5% in

specimens 217 and 219, respectively. Fe contents decrease from 37.7% to 0.8% and from 38.5% to 0.6% in specimens 217 and 219, respectively. O concentrations increase from 40.0% to 50.2% and from 38.8% to 50.6% in specimens 217 and 219, respectively. Ti and O diffuse toward the lamellae (to the right) and Fe is diffusing away from the lamellae (to the left). Error in all measurements is < 2 atomic %.

**Figure 7: Schematic representation of different possibilities for capturing exsolution lamellae in APT tips, and the implications for measuring lamellar spacing ( $\lambda$ ).**

**Table 1. Atom probe tomography data acquisition settings and run summary.**

**Table 2. Atom probe tomography bulk compositional data for all analyzed specimens.**

**Movie 1. 3D elemental isoconcentration reconstruction of specimen 219, showing intralamellar concentrations of Fe < 30.0% in blue, Ti > 25.0% in yellow, and O < 51.5% in purple, and rotated 360° along the longitudinal (z) axis.**

## DISCUSSION:

3D APT data reconstructions allow a precise measurement of the interlamellar spacing in the analyzed crystal at a resolution three orders of magnitude higher than those measured from conventional SEM images. This indicates that atomic variations in chemistry occur over a spatial extent three orders of magnitude smaller than optically observable mineralogical changes. Also, the measured interlamellar distances (29 nm and 14 nm), are consistent with the length scale for oxyexsolution as opposed to that for nucleation and growth of a separate phase, the latter of which occurs over length scales an order of magnitude greater<sup>19-20</sup>. Oxyexsolution of the titanomagnetite examined here may have resulted from either heating of the magma within the chamber due to mingling events, or oxidation induced by atmospheric exposure during ascent through the conduit and emplacement at the vent. The titanomagnetite crystal used in this study displays numerous lamellae on the order of 10  $\mu\text{m}$  or less in diameter, indicating sufficient time for partial exsolution of the entire 0.06 mm<sup>2</sup> crystal. That observation, in conjunction with the ash-venting origin of the sample, suggests that the lamellae were formed from oxidation of the lava dome following emplacement at the vent.

[Place Figure 7 here]

These measurements of the interlamellar spacing were only possible in two of the four tips analyzed and this sampling bias could induce error. As we only analyze nanoscale volumes of the crystals, each tip could capture partial representation of the distribution of lamellae, potentially leading to an erroneous calculation of interlamellar spacing ( $\lambda$ ) (**Figure 7**). Nevertheless, with the analysis of sufficient tips and the 3D tomography capabilities of APT, our approach provides a novel method to precisely measure  $\lambda$ , which can be fundamental to understand a variety of igneous and metamorphic processes. For example, analysis of Fe-Ti diffusion in magnetite crystals has been used to characterize magma mingling events and changes in magma temperature at Soufrière Hills Volcano<sup>19</sup>. The interdiffusion rate of Fe and Ti could be modeled

from accurate measurements of the interlamellar spacing if the timescale of diffusion can be constrained. Previous studies have utilized exsolution lamellae to deduce cooling rates in igneous intrusions<sup>21-22</sup>, and the novel approach of using APT can potentially be utilized to constrain element interdiffusion and improve calculations of magma and lava dome temperatures in active volcanic systems<sup>23-24</sup>. Besides the precise measurement of 3D structures at nanoscale, APT provides chemical information at the atomic scale for the same spatial resolution. This has resulted in demonstrating that the transition from titanomagnetite to ilmenite is gradual and smooth (**Figure 6**). This is in contrast to previous studies suggesting sharp and distinct contacts between the exsolving lamellae and the host phase, based on microscopy observations (SEM and TEM) without the chemical information. Consequently, only the addition of APT can accurately provide the geochemical characteristics of these phase transitions.

Atom probe tomography (APT) is still an emerging technique for geological applications<sup>25</sup>, yet our case study demonstrates the usefulness of applying this approach for the study of exsolution lamellae, quite common in minerals hosted in igneous and metamorphic rocks. In particular for understanding volcanic processes, future studies can examine multiple samples with exsolution lamellae throughout lava domes (derived from either ash venting episodes or dome collapse events) in order to better constrain variations in temperature during eruptive episodes with calculated diffusion rates.

#### **ACKNOWLEDGMENTS:**

This work was supported by funding from the National Science Foundation (NSF) through grants EAR-1560779 and EAR-1647012, the Office of the VP for Research and Economic Development, the College of Arts and Sciences, and the Department of Geological Sciences. Authors also acknowledge Chiara Cappelli, Rich Martens and Johnny Goodwin for technical assistance and the Montserrat Volcano Observatory for providing the ash samples.

#### **DISCLOSURES:**

The authors have nothing to disclose.

#### **REFERENCES:**

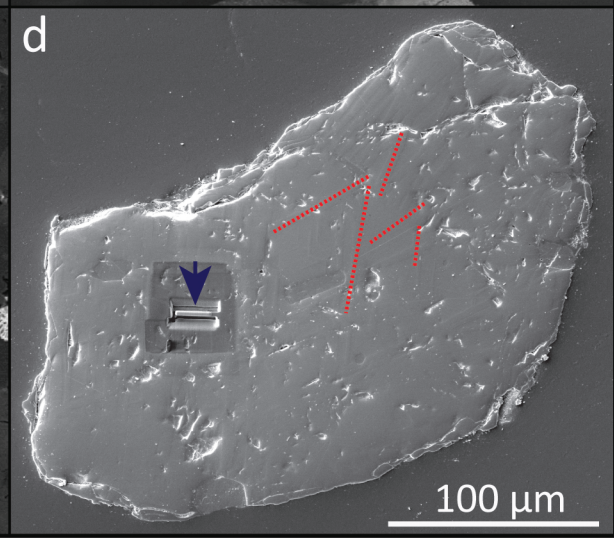
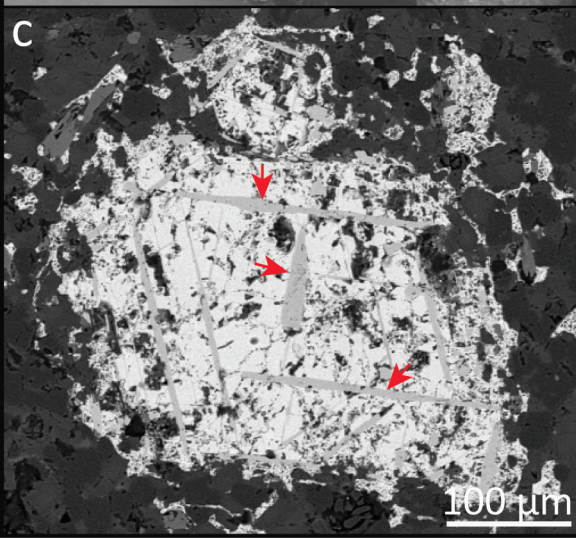
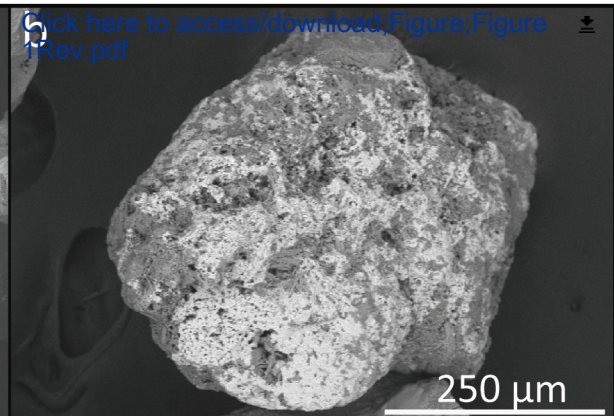
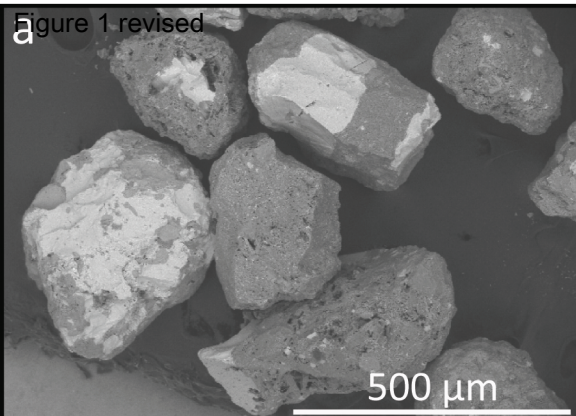
1. Kasama, T., Golla-Schindler, U., Putnis, A. High-resolution and energy-filtered TEM of the interface between hematite and ilmenite exsolution lamellae: Relevance to the origin of lamellar magnetism. *American Mineralogist*. **88**, 1190-1196 (2003).
2. Hofer, F., Wabichler, P., Grogger, W. Imaging of nanometer-sized precipitates in solids by electron spectroscopic imaging. *Ultramicroscopy*. **59**, 15–31 (1995).
3. Golla, U., Putnis, A. Valence state mapping and quantitative electron spectroscopic imaging of exsolution in titanohematite by energy-filtered TEM. *Physics and Chemistry of Minerals*. **28**, 119-129 (2001).
4. Wang, R. C., et al. Cassiterite exsolution with ilmenite lamellae in magnetite from the Huashan metaluminous tin granite in southern China. *Mineralogy and Petrology*. **105**, 71-84 (2012).

- 394 5. Robinson, P., Gordon L. Nord, M. R., Smyth, J. R., Jaffe, H.W. Exsolution lamellae in augite  
395 and pigeonite: fossil indicators of lattice parameters at high temperature and pressure.  
396 *American Mineralogist*. **62**, 857-873 (1977).
- 397 6. Austrheim, H., et al. Fragmentation of wall rock garnets during deep crustal earthquakes.  
398 *Science Advances*. **3**, e1602067 (2017).
- 399 7. Kelly, T. F., Larson, D. J. Atom probe tomography 2012. *Annual Review of Materials*  
400 *Research*. **42**, 1-31 (2012).
- 401 8. Gordon, L. M., Joester, D. Nanoscale chemical tomography of buried organic-inorganic  
402 interfaces in the chiton tooth. *Nature*. **469**, 194-197 (2011).
- 403 9. Valley, J. W., et al. Hadean age for a post-magma-ocean zircon confirmed by atom-probe  
404 tomography. *Nature Geoscience*. **7**, 219-223 (2014).
- 405 10. Pérez-Huerta, A., Laiginhas, F., Reinhard, D. A., Prosa, T. J., Martens, R. L. Atom probe  
406 tomography (APT) of carbonate minerals. *Micron*. **80**, 83-89 (2016).
- 407 11. Weber, J., et al. Nano-structural features of barite crystals observed by electron microscopy  
408 and atom probe tomography. *Chemical Geology*. **424**, 51-59 (2016).
- 409 12. Fougereuse, D., et al. Nanoscale gold clusters in arsenopyrite controlled by growth rate not  
410 concentration: Evidence from atom probe microscopy. *American Mineralogist*. **101**, 1916-  
411 1919 (2016).
- 412 13. Peterman, E. M., et al. Nanogeochronology of discordant zircon measured by atom probe  
413 microscopy of Pb-enriched dislocation loops. *Science Advances*. **2**, e1601318 (2016).
- 414 14. Cole, P. D., et al. Ash venting occurring both prior to and during lava extrusion at Soufriere  
415 Hills Volcano, Montserrat, from 2005 to 2010. *Geological Society, London, Memoirs*. **39**, 71-  
416 92 (2014).
- 417 15. Thompson, G.B., et al. In situ site-specific specimen preparation for atom probe  
418 tomography. *Ultramicroscopy*. **107**, 131-139 (2007).
- 419 16. Haggerty, S. E. Oxide textures; a mini-atlas. *Reviews in Mineralogy and Geochemistry*. **25**,  
420 129-219 (1991).
- 421 17. Gault, B., Moody, M. M., Cairney, J. M., Ringer, S. P. Atom Probe Microscopy. *Springer Series*  
422 *in Material Sciences*. **160**, 1-396 (2012).
- 423 18. Larson, D. J., Prosa, T. J., Ulfing, R. M., Geiser, B. P., Kelly, T. F. *Local Electrode Atom Probe*  
424 *Tomography: A User's Guide*. Springer, New York, 318 pp. (2013).
- 425 19. Devine, J. D., Rutherford, M. J., Norton, G. E., Young, S. R. Magma storage region processes  
426 inferred from geochemistry of Fe-Ti oxides in andesitic magma, Soufriere Hills Volcano,  
427 Montserrat, WI. *Journal of Petrology*. **44**, 1375-1400 (2003).
- 428 20. Jackson, M., Bowles, J. A. Curie temperatures of titanomagnetite in ignimbrites: Effects of  
429 emplacement temperatures, cooling rates, exsolution, and cation ordering. *Geochemistry,*  
430 *Geophysics, Geosystems*. **15**, 4343-4368 (2014).
- 431 21. Harrison, R. J., Putnis, A. The magnetic properties and crystal chemistry of oxide spinel solid  
432 solutions. *Surveys in Geophysics*. **19**, 461-520 (1998).
- 433 22. Price, G. D. Microstructures in titanomagnetites as guides to cooling rates of a Swedish  
434 intrusion. *Geological Magazine*. **116**, 313-318 (1979).
- 435 23. Price, G. D. Exsolution in titanomagnetites as an indicator of cooling rates. *Mineralogical*  
436 *Magazine*. **46**, 19-25 (1982).



- 437 24. Kuhlman, K. R., Martens, R. L., Kelly, T. F., Evans, N. D., Miller, M. K. Fabrication of  
438 specimens of metamorphic magnetite crystals for field ion microscopy and atom probe  
439 microanalysis. *Ultramicroscopy*. **89**, 169-176 (2001).
- 440 25. Dégi, J., Abart, R., Török, K., Rhede, D., Petrishcheva, E. Evidence for xenolith–host basalt  
441 interaction from chemical patterns in Fe–Ti-oxides from mafic granulite xenoliths of the  
442 Bakony–Balaton Volcanic field (W-Hungary). *Mineralogy and Petrology* **95**, 219-234 (2009).
- 443 26. Saxey, D. W., Moser, D. E., Piazzolo, S., Reddy, S. M., Valley, J. W. Atomic worlds: Current  
444 state and future of atom probe tomography in geoscience. *Scripta Materialia*. **148**, 115-121  
445 (2018).

Figure 1 revised



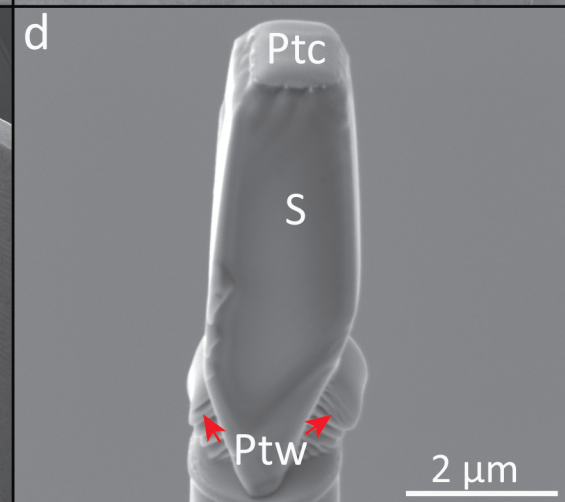
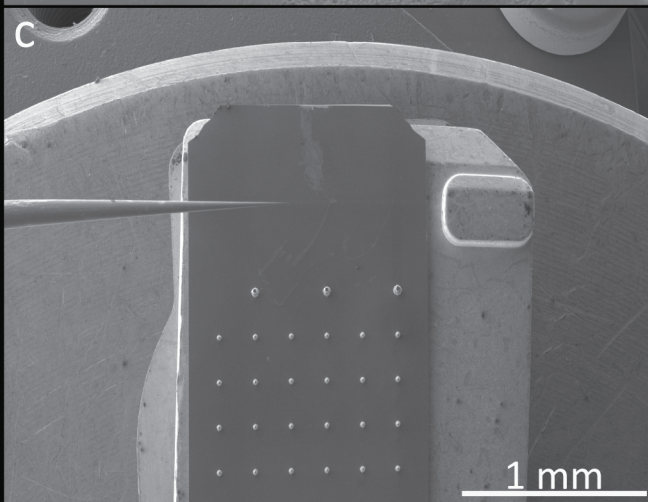
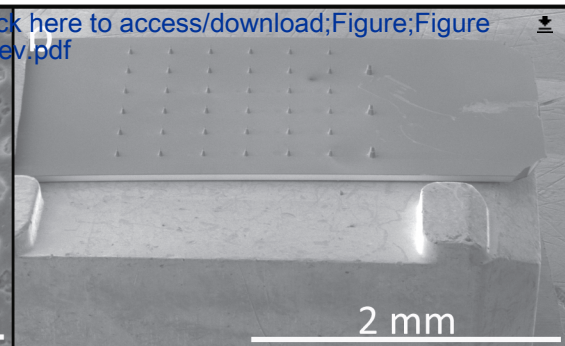
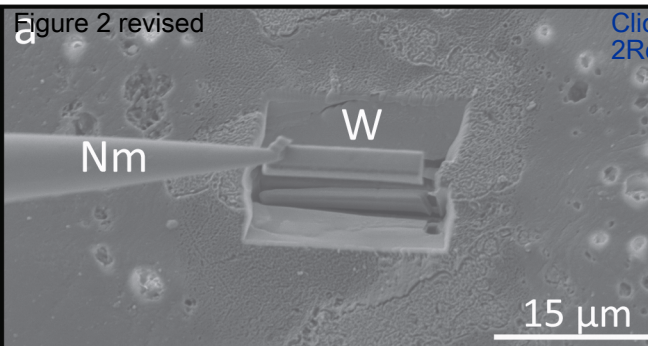
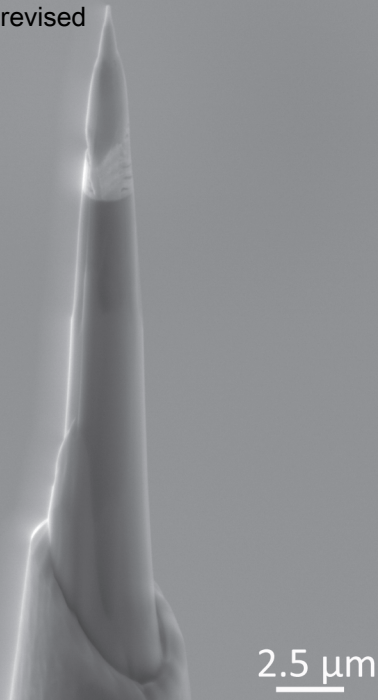
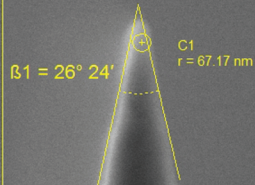


Figure 3 revised



[Click here to access/download;Figure;Figure 3Rev.pdf](#)



1 μm

Figure 4 revised

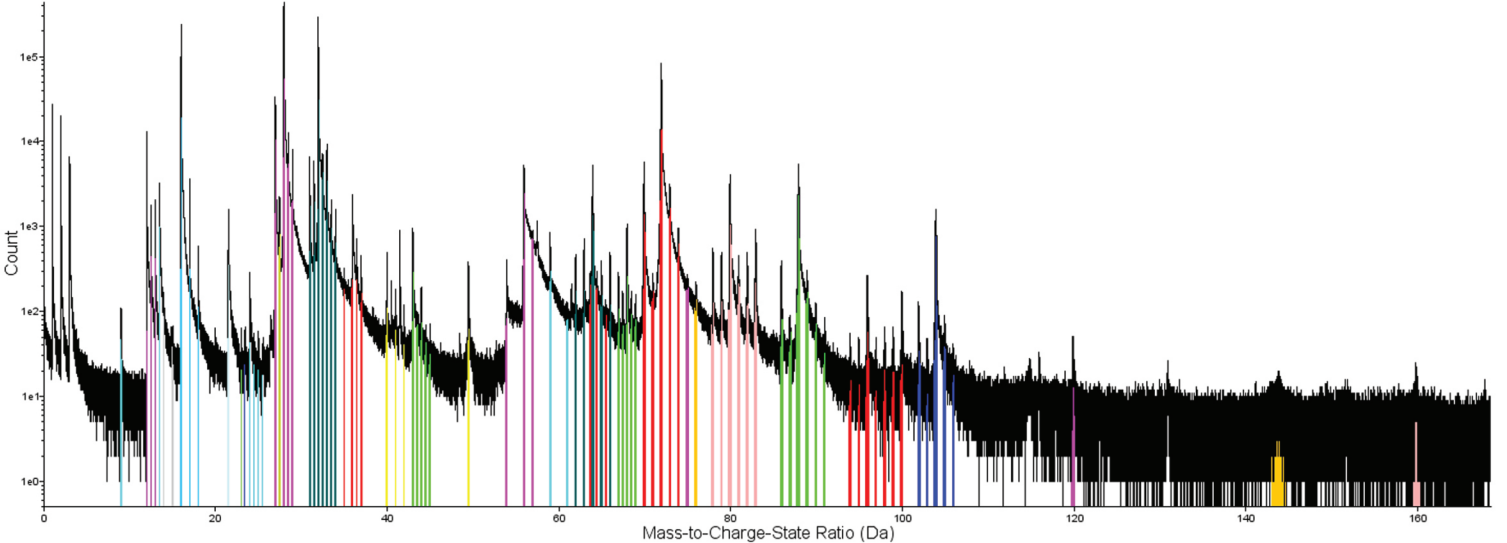
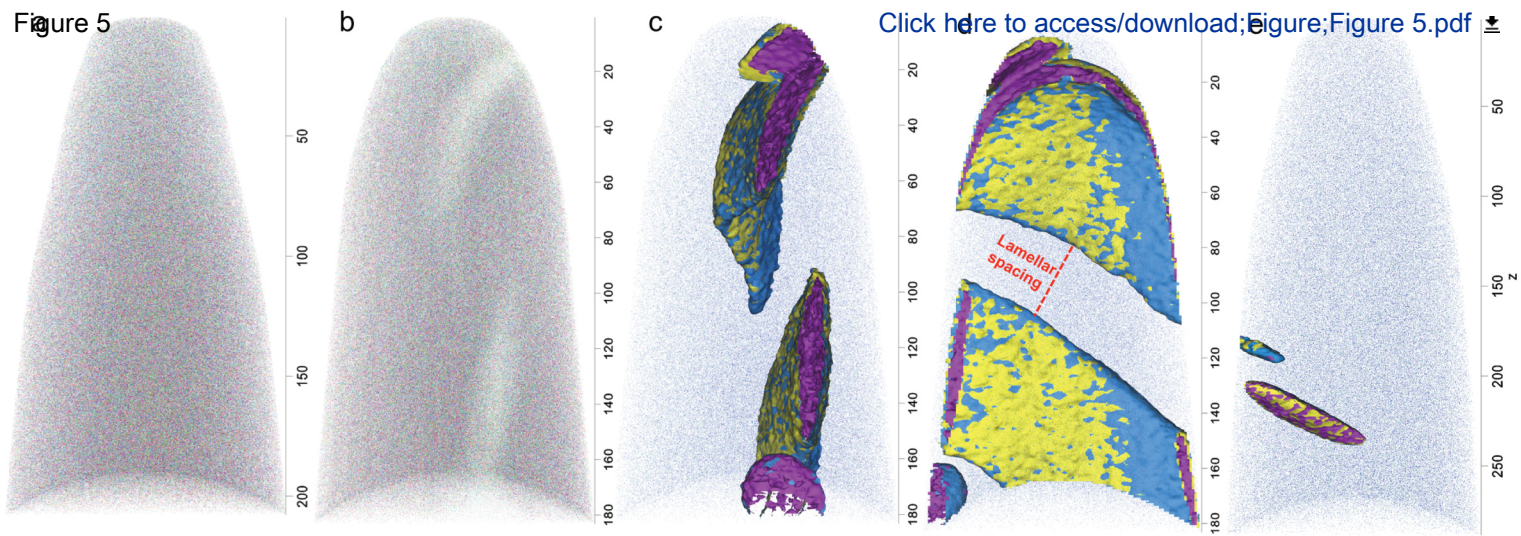




Figure 5



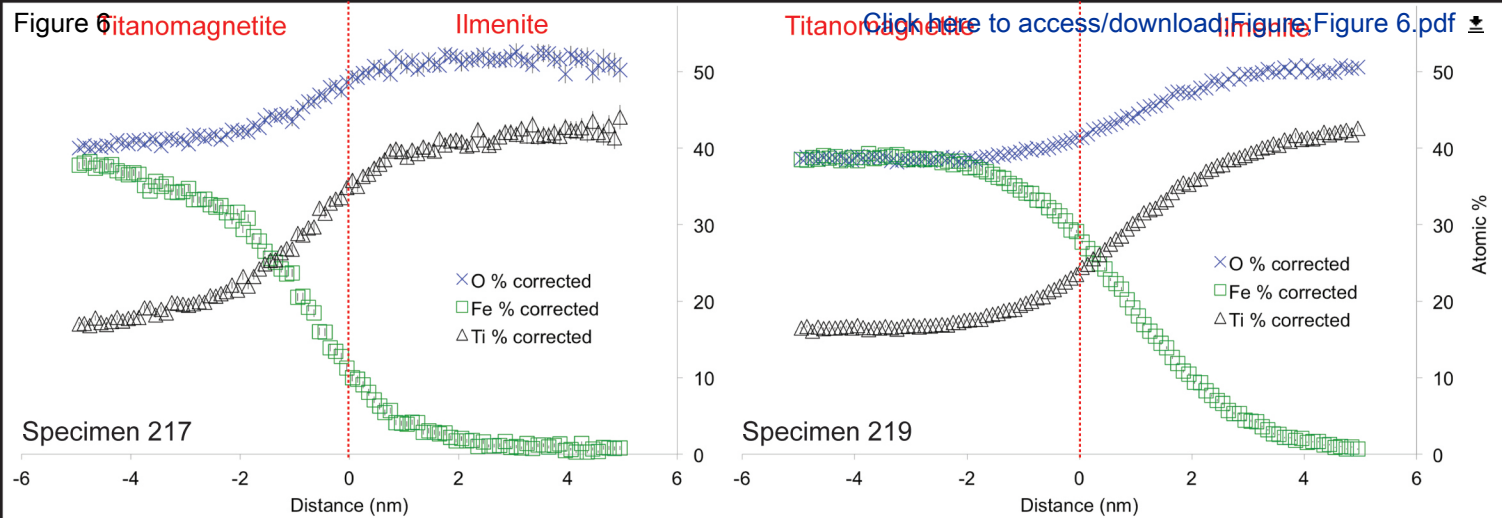
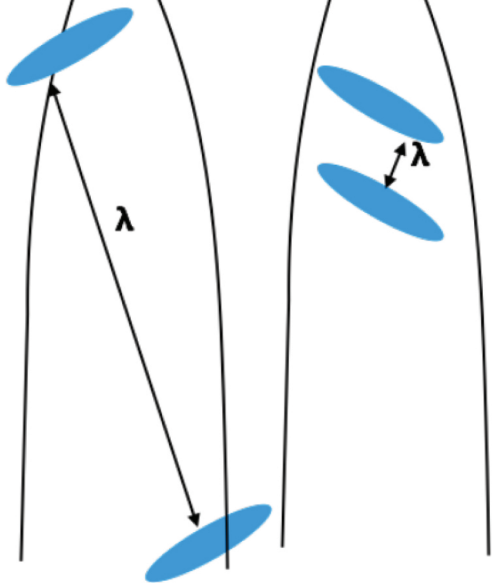


Figure 7

[Click here to  
access/download;](#)







**Table 1.** Atom Probe Tomography data acquisition settings and run summary.

Specimen	207	217
Sample Description	SHV Magnetite	SHV Magnetite
Instrument Model	LEAP 5000 XS	LEAP 5000 XS
<b>Instrument Settings</b>		
Laser Wavelength	355 nm	355 nm
Laser Pulse Rate	60 pJ	30 pJ
Laser Pulse Energy	500 kHz	500 kHz
Evaporation Control	Detection Rate	Detection Rate
Target Detection Rate (%)	0.5	0.5
Nominal Flight Path (mm)	100	100
Temperature (K)	50	50
Pressure (Torr)	$5.7 \times 10^{-11}$	$6.0 \times 10^{-11}$
ToF offset, $t_0$ (ns)	279.94	279.94
<b>Data Analysis</b>		
Software	IVAS 3.6.12	IVAS 3.6.12
Total Ions:	26,189,967	92,045,430
<i>Single</i>	15,941,806	55,999,564
<i>Multiple</i>	9,985,564	35,294,528
<i>Partial</i>	262,597	751,338
Reconstructed Ions:	25,173,742	89,915,256
<i>Ranged</i>	16,053,253	61,820,803
<i>Unranged</i>	9,120,489	28,094,453
Background (ppm/nsec)	12	12
<b>Reconstruction</b>		
Final tip state	Fractured	Fractured
Pre-/Post-analysis Imaging	SEM/n.a.	SEM/n.a.
Radius Evolution Model	"voltage"	"voltage"
$V_{\text{initial}}$ ; $V_{\text{final}}$	2205 V; 6413 V	2361 V; 7083 V

218	219
SHV Magnetite	SHV Magnetite
LEAP 5000 XS	LEAP 5000 XS
355 nm	355 nm
30 pJ	30 pJ
500 kHz	500 kHz
Detection Rate	Detection Rate
0.5	0.5
100	100
50	50
$6.1 \times 10^{-11}$	$6.1 \times 10^{-11}$
279.94	279.94
IVAS 3.6.12	IVAS 3.6.12
40,013,656	40,016,543
24,312,784	23,965,867
15,331,670	15,716,119
369,202	334,557
38,415,309	39,120,141
25,859,574	26,598,745
12,555,735	12,521,396
12	12
Fractured	Fractured
SEM/n.a.	SEM/n.a.
“voltage”	“voltage”
2198 V; 6154 V	2356 V; 6902 V

**Table 2.** APT background corrected values for atomic % of elements.

Specimen				217		
207						
Element	Atom count	Atomic %	1 $\sigma$ error	Atom count	Atomic %	1 $\sigma$ error
O	9459276	40.263	0.0155	36679256	40.724	0.0080
Fe	9424298	40.114	0.0155	35948593	39.913	0.0079
Mn	15954	0.068	0.0005	72884	0.081	0.0003
Mg	123755	0.527	0.0015	486732	0.540	0.0008
Al	85598	0.364	0.0013	329602	0.366	0.0006
Si	13855	0.059	0.0005	39307	0.044	0.0002
Na	166	0.001	0.0001	1254	0.001	0.0000
Ti	4360052	18.558	0.0097	16478946	18.296	0.0049
H	10657	0.045	0.0004	30522	0.034	0.0002
<b>Total</b>	23493611	100.00	0.04	90067097	100.00	0.02
Fe+Ti+O		98.94		98.93		
Fe/Ti		2.16		2.18		

218			219		
Atom count	Atomic %	1 $\sigma$ error	Atom count	Atomic %	1 $\sigma$ error
15396155	41.010	0.0124	16212281	41.224	0.0122
14829905	39.502	0.0121	15006853	38.159	0.0116
28166	0.075	0.0004	31450	0.080	0.0005
203596	0.542	0.0012	234231	0.596	0.0012
134637	0.359	0.0010	154779	0.394	0.0010
16278	0.043	0.0003	25750	0.065	0.0004
447	0.001	0.0001	1468	0.004	0.0001
6920481	18.434	0.0076	7645849	19.442	0.0077
12899	0.034	0.0003	14478	0.037	0.0003
37542563	100.00	0.04	39327140	100.00	0.03
98.95			98.82		
2.14			1.96		

Name of Material/Equipment	Company	Catalog Number	Comments/Description
InTouchScope Secondary Electron Microscope (SEM)	JEOL	JSM-6010PLUS/LA	
Focus Ion Beam (FIB) Secondary Electron Microscope (SEM)	TESCAN	LYRA XMU	
Local Electrode Atom Probe (LEAP)	CAMECA	5000 XS	
Integrated Visualization and Analysis Software (IVAS, version 3.6.12).			processing software



# ARTICLE AND VIDEO LICENSE AGREEMENT

Title of Article:

Protocol for Atom Probe Tomography (APT) Analysis of Exsolved Mineral Phases

Author(s):

Kimberly Genereux, Alberto Perez-Huerta, Fernando Laiginhas

Item 1: The Author elects to have the Materials be made available (as described at <http://www.jove.com/publish>) via:

☒ Standard Access

☐ Open Access

Item 2: Please select one of the following items:

☒ The Author is **NOT** a United States government employee.

☐ The Author is a United States government employee and the Materials were prepared in the course of his or her duties as a United States government employee.

☐ The Author is a United States government employee but the Materials were NOT prepared in the course of his or her duties as a United States government employee.

## ARTICLE AND VIDEO LICENSE AGREEMENT

1. **Defined Terms.** As used in this Article and Video License Agreement, the following terms shall have the following meanings: **"Agreement"** means this Article and Video License Agreement; **"Article"** means the article specified on the last page of this Agreement, including any associated materials such as texts, figures, tables, artwork, abstracts, or summaries contained therein; **"Author"** means the author who is a signatory to this Agreement; **"Collective Work"** means a work, such as a periodical issue, anthology or encyclopedia, in which the Materials in their entirety in unmodified form, along with a number of other contributions, constituting separate and independent works in themselves, are assembled into a collective whole; **"CRC License"** means the Creative Commons Attribution-Non Commercial-No Derivs 3.0 Unported Agreement, the terms and conditions of which can be found at: <http://creativecommons.org/licenses/by-nc-nd/3.0/legalcode>; **"Derivative Work"** means a work based upon the Materials or upon the Materials and other pre-existing works, such as a translation, musical arrangement, dramatization, fictionalization, motion picture version, sound recording, art reproduction, abridgment, condensation, or any other form in which the Materials may be recast, transformed, or adapted; **"Institution"** means the institution, listed on the last page of this Agreement, by which the Author was employed at the time of the creation of the Materials; **"JoVE"** means MyJoVE Corporation, a Massachusetts corporation and the publisher of The Journal of Visualized Experiments; **"Materials"** means the Article and / or the Video; **"Parties"** means the Author and JoVE; **"Video"** means any video(s) made by the Author, alone or in conjunction with any other parties, or by JoVE or its affiliates or agents, individually or in collaboration with the Author or any other parties, incorporating all or any portion

of the Article, and in which the Author may or may not appear.

2. **Background.** The Author, who is the author of the Article, in order to ensure the dissemination and protection of the Article, desires to have the JoVE publish the Article and create and transmit videos based on the Article. In furtherance of such goals, the Parties desire to memorialize in this Agreement the respective rights of each Party in and to the Article and the Video.

3. **Grant of Rights in Article.** In consideration of JoVE agreeing to publish the Article, the Author hereby grants to JoVE, subject to **Sections 4 and 7** below, the exclusive, royalty-free, perpetual (for the full term of copyright in the Article, including any extensions thereto) license (a) to publish, reproduce, distribute, display and store the Article in all forms, formats and media whether now known or hereafter developed (including without limitation in print, digital and electronic form) throughout the world, (b) to translate the Article into other languages, create adaptations, summaries or extracts of the Article or other Derivative Works (including, without limitation, the Video) or Collective Works based on all or any portion of the Article and exercise all of the rights set forth in (a) above in such translations, adaptations, summaries, extracts, Derivative Works or Collective Works and (c) to license others to do any or all of the above. The foregoing rights may be exercised in all media and formats, whether now known or hereafter devised, and include the right to make such modifications as are technically necessary to exercise the rights in other media and formats. If the "Open Access" box has been checked in **Item 1** above, JoVE and the Author hereby grant to the public all such rights in the Article as provided in, but subject to all limitations and requirements set forth in, the CRC License.

4. **Retention of Rights in Article.** Notwithstanding the exclusive license granted to JoVE in **Section 3** above, the Author shall, with respect to the Article, retain the non-exclusive right to use all or part of the Article for the non-commercial purpose of giving lectures, presentations or teaching classes, and to post a copy of the Article on the Institution's website or the Author's personal website, in each case provided that a link to the Article on the JoVE website is provided and notice of JoVE's copyright in the Article is included. All non-copyright intellectual property rights in and to the Article, such as patent rights, shall remain with the Author.

5. **Grant of Rights in Video – Standard Access.** This **Section 5** applies if the "Standard Access" box has been checked in **Item 1** above or if no box has been checked in **Item 1** above. In consideration of JoVE agreeing to produce, display or otherwise assist with the Video, the Author hereby acknowledges and agrees that, Subject to **Section 7** below, JoVE is and shall be the sole and exclusive owner of all rights of any nature, including, without limitation, all copyrights, in and to the Video. To the extent that, by law, the Author is deemed, now or at any time in the future, to have any rights of any nature in or to the Video, the Author hereby disclaims all such rights and transfers all such rights to JoVE.

6. **Grant of Rights in Video – Open Access.** This **Section 6** applies only if the "Open Access" box has been checked in **Item 1** above. In consideration of JoVE agreeing to produce, display or otherwise assist with the Video, the Author hereby grants to JoVE, subject to **Section 7** below, the exclusive, royalty-free, perpetual (for the full term of copyright in the Article, including any extensions thereto) license (a) to publish, reproduce, distribute, display and store the Video in all forms, formats and media whether now known or hereafter developed (including without limitation in print, digital and electronic form) throughout the world, (b) to translate the Video into other languages, create adaptations, summaries or extracts of the Video or other Derivative Works or Collective Works based on all or any portion of the Video and exercise all of the rights set forth in (a) above in such translations, adaptations, summaries, extracts, Derivative Works or Collective Works and (c) to license others to do any or all of the above. The foregoing rights may be exercised in all media and formats, whether now known or hereafter devised, and include the right to make such modifications as are technically necessary to exercise the rights in other media and formats. For any Video to which this **Section 6** is applicable, JoVE and the Author hereby grant to the public all such rights in the Video as provided in, but subject to all limitations and requirements set forth in, the CRC License.

7. **Government Employees.** If the Author is a United States government employee and the Article was prepared in the course of his or her duties as a United States government employee, as indicated in **Item 2** above, and any of the licenses or grants granted by the Author hereunder exceed the scope of the 17 U.S.C. 403, then the rights granted hereunder shall be limited to the maximum

rights permitted under such statute. In such case, all provisions contained herein that are not in conflict with such statute shall remain in full force and effect, and all provisions contained herein that do so conflict shall be deemed to be amended so as to provide to JoVE the maximum rights permissible within such statute.

8. **Protection of the Work.** The Author(s) authorize JoVE to take steps in the Author(s) name and on their behalf if JoVE believes some third party could be infringing or might infringe the copyright of either the Author's Article and/or Video.

9. **Likeness, Privacy, Personality.** The Author hereby grants JoVE the right to use the Author's name, voice, likeness, picture, photograph, image, biography and performance in any way, commercial or otherwise, in connection with the Materials and the sale, promotion and distribution thereof. The Author hereby waives any and all rights he or she may have, relating to his or her appearance in the Video or otherwise relating to the Materials, under all applicable privacy, likeness, personality or similar laws.

10. **Author Warranties.** The Author represents and warrants that the Article is original, that it has not been published, that the copyright interest is owned by the Author (or, if more than one author is listed at the beginning of this Agreement, by such authors collectively) and has not been assigned, licensed, or otherwise transferred to any other party. The Author represents and warrants that the author(s) listed at the top of this Agreement are the only authors of the Materials. If more than one author is listed at the top of this Agreement and if any such author has not entered into a separate Article and Video License Agreement with JoVE relating to the Materials, the Author represents and warrants that the Author has been authorized by each of the other such authors to execute this Agreement on his or her behalf and to bind him or her with respect to the terms of this Agreement as if each of them had been a party hereto as an Author. The Author warrants that the use, reproduction, distribution, public or private performance or display, and/or modification of all or any portion of the Materials does not and will not violate, infringe and/or misappropriate the patent, trademark, intellectual property or other rights of any third party. The Author represents and warrants that it has and will continue to comply with all government, institutional and other regulations, including, without limitation all institutional, laboratory, hospital, ethical, human and animal treatment, privacy, and all other rules, regulations, laws, procedures or guidelines, applicable to the Materials, and that all research involving human and animal subjects has been approved by the Author's relevant institutional review board.

11. **JoVE Discretion.** If the Author requests the assistance of JoVE in producing the Video in the Author's facility, the Author shall ensure that the presence of JoVE employees, agents or independent contractors is in accordance with the relevant regulations of the Author's institution. If more than one author is listed at the beginning of this Agreement, JoVE may, in its sole



## ARTICLE AND VIDEO LICENSE AGREEMENT

discretion, elect not take any action with respect to the Article until such time as it has received complete, executed Article and Video License Agreements from each such author. JoVE reserves the right, in its absolute and sole discretion and without giving any reason therefore, to accept or decline any work submitted to JoVE. JoVE and its employees, agents and independent contractors shall have full, unfettered access to the facilities of the Author or of the Author's institution as necessary to make the Video, whether actually published or not. JoVE has sole discretion as to the method of making and publishing the Materials, including, without limitation, to all decisions regarding editing, lighting, filming, timing of publication, if any, length, quality, content and the like.

12. **Indemnification.** The Author agrees to indemnify JoVE and/or its successors and assigns from and against any and all claims, costs, and expenses, including attorney's fees, arising out of any breach of any warranty or other representations contained herein. The Author further agrees to indemnify and hold harmless JoVE from and against any and all claims, costs, and expenses, including attorney's fees, resulting from the breach by the Author of any representation or warranty contained herein or from allegations or instances of violation of intellectual property rights, damage to the Author's or the Author's institution's facilities, fraud, libel, defamation, research, equipment, experiments, property damage, personal injury, violations of institutional, laboratory, hospital, ethical, human and animal treatment, privacy or other rules, regulations, laws, procedures or guidelines, liabilities and other losses or damages related in any way to the submission of work to JoVE, making of videos by JoVE, or publication in JoVE or elsewhere by JoVE. The Author shall be responsible for, and shall hold JoVE harmless from, damages caused by lack of sterilization, lack of cleanliness or by contamination due to


the making of a video by JoVE its employees, agents or independent contractors. All sterilization, cleanliness or decontamination procedures shall be solely the responsibility of the Author and shall be undertaken at the Author's expense. All indemnifications provided herein shall include JoVE's attorney's fees and costs related to said losses or damages. Such indemnification and holding harmless shall include such losses or damages incurred by, or in connection with, acts or omissions of JoVE, its employees, agents or independent contractors.

13. **Fees.** To cover the cost incurred for publication, JoVE must receive payment before production and publication of the Materials. Payment is due in 21 days of invoice. Should the Materials not be published due to an editorial or production decision, these funds will be returned to the Author. Withdrawal by the Author of any submitted Materials after final peer review approval will result in a US\$1,200 fee to cover pre-production expenses incurred by JoVE. If payment is not received by the completion of filming, production and publication of the Materials will be suspended until payment is received.

14. **Transfer, Governing Law.** This Agreement may be assigned by JoVE and shall inure to the benefits of any of JoVE's successors and assignees. This Agreement shall be governed and construed by the internal laws of the Commonwealth of Massachusetts without giving effect to any conflict of law provision thereunder. This Agreement may be executed in counterparts, each of which shall be deemed an original, but all of which together shall be deemed to be one and the same agreement. A signed copy of this Agreement delivered by facsimile, e-mail or other means of electronic transmission shall be deemed to have the same legal effect as delivery of an original signed copy of this Agreement.

A signed copy of this document must be sent with all new submissions. Only one Agreement is required per submission.

### CORRESPONDING AUTHOR

Name:	Alberto Perez-Huerta	
Department:	Geological Sciences	
Institution:	University of Alabama	
Title:	Associate Professor	
Signature:		Date: 02/19/2019

Please submit a **signed** and **dated** copy of this license by one of the following three methods:

1. Upload an electronic version on the JoVE submission site
2. Fax the document to +1.866.381.2236
3. Mail the document to JoVE / Attn: JoVE Editorial / 1 Alewife Center #200 / Cambridge, MA 02140

